

Removal of ammoniacal nitrogen from contaminated groundwater using waste foundry sand in the permeable reactive barrier

Ayad A.H. Faisal^{a,*}, Laith A. Naji^a, Anis Ahmad Chaudhary^b, B. Saleh^c

^aDepartment of Environmental Engineering, College of Engineering, University of Baghdad, Baghdad, Iraq, Tel. +9647904208688; emails: ayadabedalhamzafaisal@yahoo.com (A.A.H. Faisal), add.ali.lith@gmail.com (L.A. Naji)

^bDepartment of Biology, College of Science, Imam Mohammad Ibn Saud Islamic University (IMSIU), Riyadh – 11623, Saudi Arabia, email: anis.chaudhary@gmail.com

^cMechanical Engineering Department, College of Engineering, Taif University, P.O. Box: 11099, Taif 21944, Saudi Arabia, email: b.saleh@tu.edu.sa

Received 29 November 2020; Accepted 11 May 2021

ABSTRACT

The focal point of this study was to use the waste foundry sand (WFS) in the remediation of simulated aqueous solution contaminated with ammonia nitrogen through batch and column tests. Recycling this waste is a real application for sustainable principles because it will reduce disposal costs and the required area in the sanitary landfill. Based on the kinetic sorption measurements for ammonia nitrogen onto WFS, the predominant mechanism was the chemisorption because the measurements were well fitted with the pseudo-second-order model. In comparison with the Freundlich model, the sorption isotherm data were well formulated by models of Langmuir and Sips with a maximum adsorption capacity of 1.152 mg/g. The breakthrough curves for a duration of 80 h certified that the two weight ratios (10:90 and 20:80) of WFS:sand were suitable for maintaining the reactivity and conductivity of permeable reactive barrier (PRB) for pollutant under consideration. The results proved that the increasing of WFS and bed depth increased the breakthrough and saturation times with the sorption capacity of the barrier. Also, the appearance of these curves was directly proportional to the inlet concentration of pollutants and the flow rate of contaminated water. Statistical measures specifically Nash–Sutcliffe efficiency and coefficient of determination were proved that the breakthrough curves were well described by Thomas, Belter, and Yan models.

Keywords: Remediation; Leachate; Sorption; Waste foundry sand; Sustainable

1. Introduction

Massive organic and inorganic species can release to the subsurface environment due to the rapid development in the agricultural and industrial fields; however, nitrogenous compounds like ammonium ($\text{NH}_4\text{-N}$) are familiar compounds detected in the groundwater [1]. Aquifers located along the surface water resources such as rivers and lakes can easily contaminate by ammonium due to the exchange

of water with such resources and this represents a potential threat to the quality of groundwater [2]. Ammonium plume has the ability to propagate in the groundwater for long extents where previous records proved that products of ammonium spilled from a fertilizer factory can reach a distance of 300 m from the spillage source. For example, ammonium was found to contaminate groundwater because of the spillage from the Leuna site (Germany) that was used as a center of the chemical industry for approximately 100 y.

* Corresponding author.

In addition, the increase of water content in the solid wastes of the sanitary landfill to exceed the field capacity could lead to the formation of complex wastewater (i.e., leachate) [3]. Nitrogenous compounds are popular contaminants in this leachate and; in many cases; the liner of sanitary landfills can fail under service. So, the leachate can cause significant damage to the quality of groundwater and this may be accompanied by critical issues for public health and the environment as recorded in many polluted sites through America, Australia, England, and Korea [4,5].

There are different technologies for removing ammonium from contaminated groundwater mentioned in the previous literature like aerated ponds with biofilm promoting mats, constructed wetlands [6–8], and soil filter systems [9]. Due to the presence of several limitations about the efficacy and performance of these methods, innovative technology must develop for remediating groundwater [10]. *In-situ* permeable reactive barrier (PRB) is received great attention as a promising technique that can be an alternative for traditional technologies [11,12]. The idea of PRB depends on the emplacement of reactive material in the continuous trench below the ground surface perpendicular to the path of the contaminant front where the water will pass and contaminants must be trapped by different reactions to obtain less toxic end-products [13].

Activated carbon, activated silica, and calcium carbonate were tested to eliminate $\text{NH}_4\text{-N}$ from contaminated water. Results proved that the nitrogen in the form of proteins was removed with efficiency ranged from 74% to 89% [14]. Removal of $\text{NH}_4\text{-N}$ from leachate using clinoptilolite-PRB was achieved in the lab-scale study and this is opened a new horizon on sustainable ammonium removal [15]. Natural zeolite was also applied in the PRB for remediation of simulated groundwater contained $\text{NH}_4\text{-N}$ and the outputs proved that the remediation process can achieve through the ion exchange mechanism [16]. To apply the concepts of sustainable development, recent studies were oriented to use byproducts of solid wastes generated from industrial activities. In this regard, researchers have been focused on the effectiveness of inexpensive materials for removing $\text{NH}_4\text{-N}$ such as refuse cement and concrete [17], activated carbon and limestone [4], and clay as well as zeolite [18]. Many studies used innovative materials for reclamation of water contaminated with heavy metals like cation-exchange resin [19–25], cement kiln dust [26], olive pips [27,28], zero-valent iron and aluminum [29,30], and others.

In Iraq, approximately 10,000 kg of WFS can generate from Nasr Company for Mechanical Industries each day and this considers a huge quantity that forms a great load on the ambient. So, it is attractive to reuse this quantity in the treatment of contaminated water to fulfill the environmental requirements and to decrease the cost of WFS disposal [31]. Hence, the aim of the study was; (i) To evaluate the ability of WFS in the removal of $\text{NH}_3\text{-N}$ from aqueous solutions, and (ii) To calculate the suitable WFS/filter sand mixture for PRB to satisfy the reactivity and permeability requirements for finding the barrier longevity in the reclamation of groundwater contaminated with $\text{NH}_3\text{-N}$.

2. Models for batch and continuous outputs

2.1. Sorption models

It is worthy to find a relationship between the quantity of contaminant retained within the solid phase (q_e) and the final concentration of contaminant remaining in the bulk solution (C_e) [32]. Mathematically, this relationship is plotted q_e with C_e at a specific temperature and it can be represented by the following models [33–36]:

- Freundlich model (1906): is the earliest isotherm model applicable for multilayer sorption onto heterogeneous surfaces and can be as follows [37]:

$$q_e = K_f C_e^{\frac{1}{n}} \quad (1)$$

where K_f is an indicator for sorption capacity of the reactive material ($\text{mg/g(L/mg)}^{1/n}$) and n is the sorption intensity.

- Langmuir model (1916): is another nonlinear isotherm model for the description of the monolayer sorption process onto homogeneous surfaces as follows [38]:

$$q_e = \frac{q_{\max} b C_e}{1 + b C_e} \quad (2)$$

where q_{\max} is the maximum adsorption capacity (mg/g) and b is the affinity between the contaminant and reactive solid.

- Sips model (1948): is a three parameters model that collected between the behaviors of Freundlich and Langmuir relationships. For sorption data at equilibrium status, this model listed in Eq. (3) (named also as “Langmuir–Freundlich model”) follows Langmuir for the higher concentration of contaminant while behavior will be according to Freundlich at lower concentration [39]:

$$q_e = \frac{K_s C_e^{\beta_s}}{a_s C_e^{\beta_s} + 1} \quad (3)$$

where K_s , a_s , and β_s are the Sips model constants.

2.2. Kinetic models and sorption mechanisms

For designing the proper sorption process, the mass transfer of contaminant from the liquid phase to solid sorbent must be predicted. This can achieve by applying the kinetics models having linearized forms as in Eqs. (4)–(6) [40]:

Pseudo-first-order:

$$q_t = q_e (1 - e^{-k_1 t}) \quad (4)$$

Pseudo-second-order:

$$q_t = \frac{t}{\left(\frac{1}{k_2 q_e^2} + \frac{t}{q_e} \right)} \quad (5)$$

Elovich:

$$q_t = \frac{1}{\beta} \ln(\alpha\beta) + \frac{1}{\beta} \ln(t) \tag{6}$$

where k_1 is the equilibrium rate constant of pseudo-first-order (1/min), k_2 is the rate constant of pseudo-second-order model (g/mg min), q_e is the equilibrium quantity of contaminant retained onto sorbent (mg/g), and q_t is the quantity of contaminant retained onto sorbent at time t (mg/g).

To identify the transport of contaminant by diffusion, the theory of intra-particle diffusion model [41] was applied based on the following empirical relationship:

$$q_i = k_i t^{0.5} + C_i \tag{7}$$

where k_i (mg/g h^{0.5}) is the rate constant for the i stage and it represents the slope of the linear plot between q_i and $t^{0.5}$, and C_i is the intercept for the i stage that reflects the thickness of the boundary layer. When this intercepts with the origin, the rate-limiting process is governed by the intra-particle diffusion only. However, additional mechanisms are involved with this diffusion for other cases (i.e., intercept not equal zero). Previous studies signified that this plot can consist of two or three portions; the first one is sharper (identical to instantaneous or external surface adsorption), the slope of the second portion may vary gradually and intra-particle diffusion can be the rate-limiting, and the last region reflects the final stage of equilibrium for intra-particle diffusion [42].

2.3. Breakthrough curves

The relationship of the contaminant normalized concentration (C/C_0) and the residence time at a certain location along the PRB bed can be described through a set of theoretical and empirical models. The advection-dispersion equation is a familiar relationship for predicting the spatial and temporal movement of the contaminant front. It can solve by analytical or numerical solutions depends on the problem complexity and available information. These solutions are validated with experimental measurements obtained from the column tests. To avoid the strict assumptions required for analytical solutions and difficult formulation for numerical solutions, simpler, and more tractable empirical expressions like Thomas, Belter, and Yan models can be applied (Table 1). These models are profitable in the designing of PRB on the field scale especially in specifying the barrier longevity through the identification of breakthrough and saturation points. There are several previous studies such as [26,33] that introduce the assumptions and concepts utilized in the derivation of models mentioned in this table.

3. Experimental work

3.1. Material

The reactive material used in the batch and continuous tests is the byproduct of solid waste named waste foundry sand (WFS) that generated from industrial activities of

Nasr Company for Mechanical Industries, Baghdad, Iraq. The physical properties of this waste are porosity, bulk density, hydraulic conductivity, cation exchange capacity, and surface area of 0.46, 1.44 g/cm³, 1×10^{-6} cm/s, 11 meq/100 g, and 5.9 m²/g respectively. Porosity represents the proportion between the volume of voids and the total volume of the bed. The Al₂O₃ and Fe₂O₃ are the main components of this waste with percentages approximately of 3 and 2 beside the silica that formed 94%; however, the size of the particles was ranged from 0.075 to 0.84 mm with the coefficient of uniformity (d_{60}/d_{10}) equal to 1.94. Foundry sand is utilized in processes of casting by iron foundries to form molds in which molten iron has been poured. The sand molds are broken after cooling and the final iron products can remove. Clay (or bentonite) as a binder with a percentage ranged from 4% to 10% is mixed with the sand to keep the mold shape during pouring and cooling [43].

The principle geotechnical properties of the reactive medium in PRB (i.e., permeability, porosity, and particle size curve) produce from the characteristics of the surrounding aquifer. Thus, the barrier should fulfill the following; (i) "retention criteria" (i.e., must be fine enough to trap loose particles of soil), (ii) "permeability criteria" (i.e., must be coarse enough to permit flow and avoid the high internal pore pressure development). Therefore, constriction size represents a useful variable to understand the migration inside the reactive medium. This size is the diameter of the largest particle capable of passing in PRB. Also, the hydraulic conductivity of the reactive medium must be at least one order of magnitude greater than that of the aquifer [44]. Because, the conductivity of WFS was very low as mentioned previously, a mixture of 60% coarse sand with 40% fine sand was thoroughly mixed with WFS in certain percentages to satisfy the required value of hydraulic conductivity for PRB. The "mean particle size, d_{50} " values of coarse and fine sand were equal to 1.65 and 1.62 mm, respectively. The particle size distribution curves proved that the filter sand consists of 100% sand while WFS contains 6% bentonite (or clay) and 94% sand; so, this clay would be responsible for foundry sand reactivity.

A certain mass of anhydrous ammonium chloride (≈3.819 g) manufactured by E. MERCK, Denmark was

Table 1
Empirical models for transport of ammonia nitrogen in the packed column

Model	Form
Thomas	$\frac{C}{C_0} = \frac{1}{1 + \exp\left[\frac{Mq_0 k_{Th}}{Q} - \frac{K_{Th} C_0 t}{1,000}\right]}$
Belter	$\frac{C}{C_0} = \frac{1}{2} \left(1 + \operatorname{erf} \left[\frac{t - t_{0.5}}{\sqrt{2\sigma t_{0.5}}} \right] \right)$
Yan	$\frac{C}{C_0} = 1 - \frac{1}{1 + \left(\left(\frac{Q \times C_0}{q_0 \cdot M} \right) \times t \right)^a}$

dissolved in 1 L of deionized water at room temperature to obtain the stock solution. This solution contained $\text{NH}_4\text{-N}$ with a concentration of 1,000 mg/L and its acidity can be adjusted by drops of 0.1 M of HCl or NaOH as needed.

3.2. Kinetic and isotherm study

Kinetic tests were conducted to investigate the variation of $\text{NH}_3\text{-N}$ removal from aqueous solutions as a function of the contact time. Seven flasks of 250 mL were prepared and 100 mL of aqueous solution contaminated with 476 mg/L of $\text{NH}_3\text{-N}$ were distributed on these flasks. The initial pH of the solution was kept at 6 and 90 g of WFS was added to each flask which were agitated by an orbital shaker (Edmund Buhler SM25, German) at 200 rpm. The choice of seven flasks aims to find the removal efficiencies of $\text{NH}_3\text{-N}$ after periods of 3, 10, 20, 30, 60, 90, and 120 min. At the end of each period, sorbent grains were filtered from the solution by filtration and the concentration of contaminant in the supernatant can measure by KJELTEC AUC 1030 analyzer using distillation and titration method that suitable for $\text{NH}_3\text{-N}$ concentration of greater than 5 mg/L. The measurements were conducted in the laboratory of Biological Science – University of Baghdad – Iraq.

Also, sorption isotherm tests were carried out to find q_e as a function of C_e as described section Sorption models. These tests require to add 20, 30, 40, 60, 70, 90, and 120 g WFS to 100 mL of water contaminated with 697 mg/L $\text{NH}_3\text{-N}$ for initial pH of 9 at agitation speed and contact time of 200 rpm and 60 min, respectively. The same procedure mentioned previously could be adopted to measure the concentration of $\text{NH}_3\text{-N}$; however, the q_e determines by:

$$q_e = (C_0 - C_e) \frac{V}{m} \quad (8)$$

where m and V are the mass (g) of WFS and volume of contaminated water (L) added to the flask, respectively.

3.3. Column tests

Three PVC columns (90 cm height and 6.3 cm inner diameter) were constructed to achieve the continuous tests. The tests were directed to specify the performance of PRB by identification the best mixture proportions of WFS and filter sand that must be packed in each column. The tests were conducted under the variation effects of inlet concentration (200, 500, and 700 mg/L), and flow rate (25, 30, and 35 mL/min) for ports 15 (P1) and 80 cm (P2) along the packed column. The tests have simulated the migration of $\text{NH}_3\text{-N}$ along the barrier bed in the one dimension under the effect of advective and longitudinal dispersive fluxes.

The choice of three columns is required to conduct three different configurations of operation at the same period especially the PRB adopted in this work composed of WFS, fine sand, and coarse sand to satisfy the hydraulic conductivity requirements. The first configuration requires to fill the column with a mixture composed of 60% coarse sand and 40% fine sand. This configuration is the reference bed (bulk density = 1.7 g/cm³, porosity = 0.32, and hydraulic

conductivity = 4.7×10^{-1} cm/s) which is applied to find the role of sand in the treatment process. Then, 90% of the reference bed was mixed with 10% WFS to produce PRB with properties of bulk density = 1.59 g/cm³, porosity = 0.36, and hydraulic conductivity = 3.9×10^{-2} cm/s. This bed represents the second configuration and can use to study the effect of reactive material on the treated water. In the third configuration, the proportion of WFS was increased to 20% where the bulk density will become 1.65 g/cm³, while porosity and hydraulic conductivity have values of 0.34 and 3.9×10^{-2} cm/s, respectively. The last configuration was aimed to give another choice for PRB in comparison with the second configuration to choose a suitable one based on the reactivity and permeability requirements.

All experiments were performed at room temperature using contaminated water with a pH of 9 for inlet concentration and volumetric feed flow rate illustrated previously. To avoid the entrapped air in the bed, contaminated water was injected from the bottom in the upward direction. Samples were taken periodically from the ports P1 and P2 for the duration not greater than 90 h to monitor the concentration of $\text{NH}_3\text{-N}$.

4. Results and discussion

4.1. Effects of operational conditions

Fig. 1a illustrates the variation of sorbed quantity (q_e) of $\text{NH}_3\text{-N}$ and removal percentages with contact time for two values of initial pH specifically 3 and 9 at C_0 and WFS dosage equal to 600 mg/L and 90 g/100 mL, respectively, for speed of 200 rpm. For pH = 3, this Fig. 1 certified that the change of contact time from 5 to 30 min caused a remarkable jump in the value of a sorbed quantity (and removal efficiency) from 0.04 (6%) to 0.38 mg/g (57%), respectively. The presence of sufficient binding sites for sorption of the contaminant in the initial times might be the cause for this behavior [45,46]. However, no significant change in the value of q_e was noticed beyond 60 min which represented the time suitable for achieving equilibrium status. In addition, this figure demonstrated that the increase of initial pH had a good ability in the improvement of removal process where for example the value of q_e increased from 0.4 to 0.487 mg/g at equilibrium when pH changed from 3 to 9, respectively. With the variation of pH, ammonia either be non-ionized ammonia (NH_3) or ionized ammonium (NH_4^+) as follows:



So, the presence of ammoniacal nitrogen in the ionized form resulted in a lower columbic repulsion and this enhanced its removal with the increasing pH [47].

Fig. 1b certified that the change of sorbent dosage from 20 to 90 g will associate with evidence variation in the removal percentages from 43% to 96%, respectively, for C_0 of 400 mg/L because of the presence of high vacant sites in the larger dosages. However, this increase of dosage for the same range was caused a decrease in q_e from 0.86 to 0.32 mg/g, respectively, because the sorbed quantity of

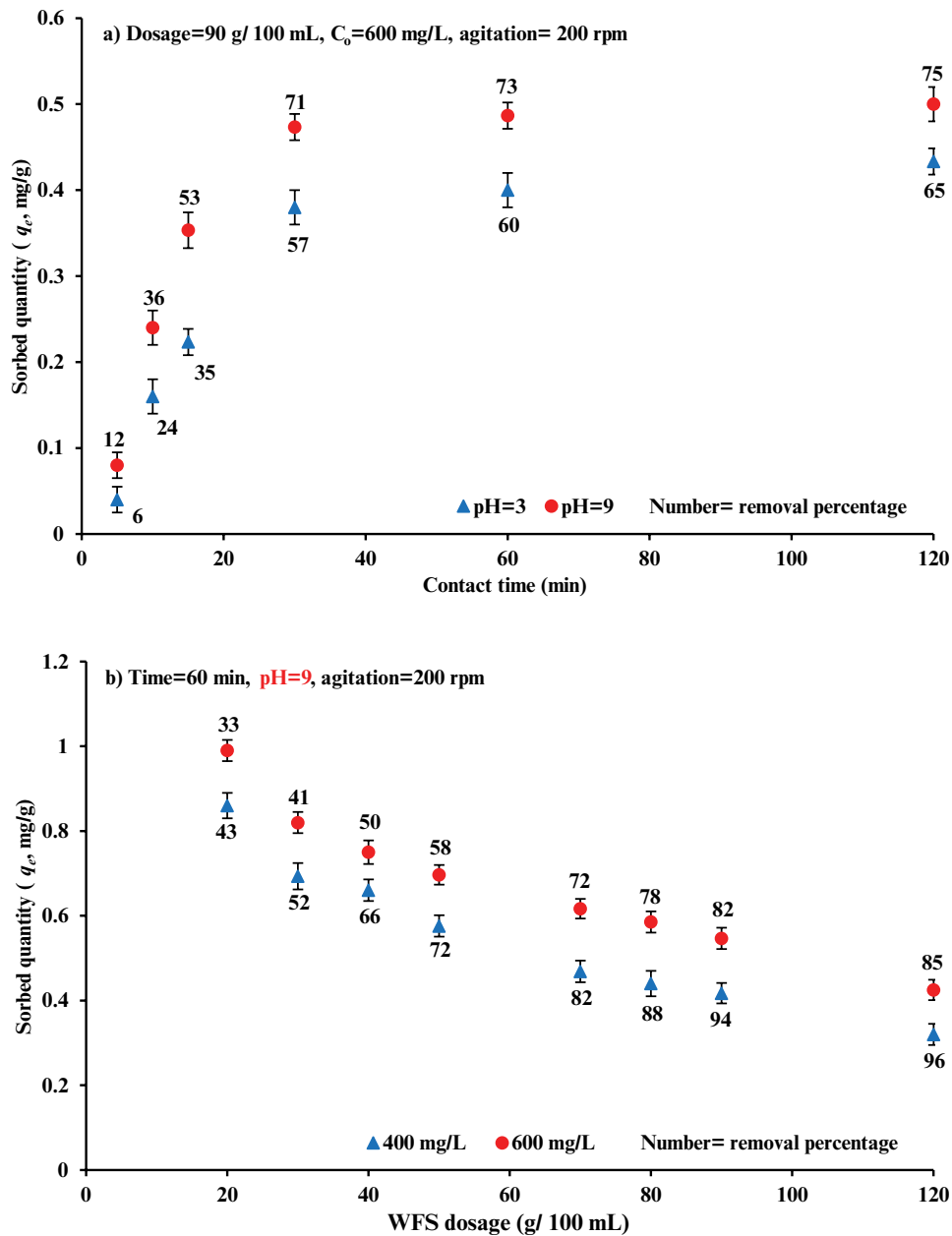


Fig. 1. Variation of NH₃-N sorbed quantity onto WFS and removal percentages with (a) residence time and acidity of aqueous solution and (b) sorbent dosage and initial concentration for agitation speed of 200 rpm.

contaminant related inversely with sorbent dosage [48]. A decrease of NH₃-N removal (an increase of sorbed quantity) due to the increase of initial concentration can be observed in the same figure. Also, it seems that the NH₃-N removed per each WFS unit mass was increased in a rapid manner at equilibrium for low initial concentration, and; then, it begins to increase with higher concentrations.

4.2. Sorption kinetics

A theoretical formulation for measured kinetic data was applied by fitting with kinetic models described in section Kinetic models and sorption mechanisms. This

fitting requires to use of the nonlinear regression option in Microsoft Excel 2016 to find the constants of kinetic models illustrated in Table 2. The concurrence between these models and experimental measurements is clear in Fig. 2a. However, the sorption process of NH₃-N onto WFS follows the pseudo-second-order model with a determination coefficient (*R*²) of 0.989, and the calculated *q_e* of 0.398 mg/g approaches from the experimental value of 0.393 mg/g. Accordingly, chemisorption is the predominant mechanism for the sorption of NH₃-N onto WFS.

Fig. 2b plots the sorbed quantity of NH₃-N at any time (*t*) with *t*^{0.5} to find the coefficient of the intra-particle diffusion model (Eq. (7)) for portions 1 and 2. This coefficient had

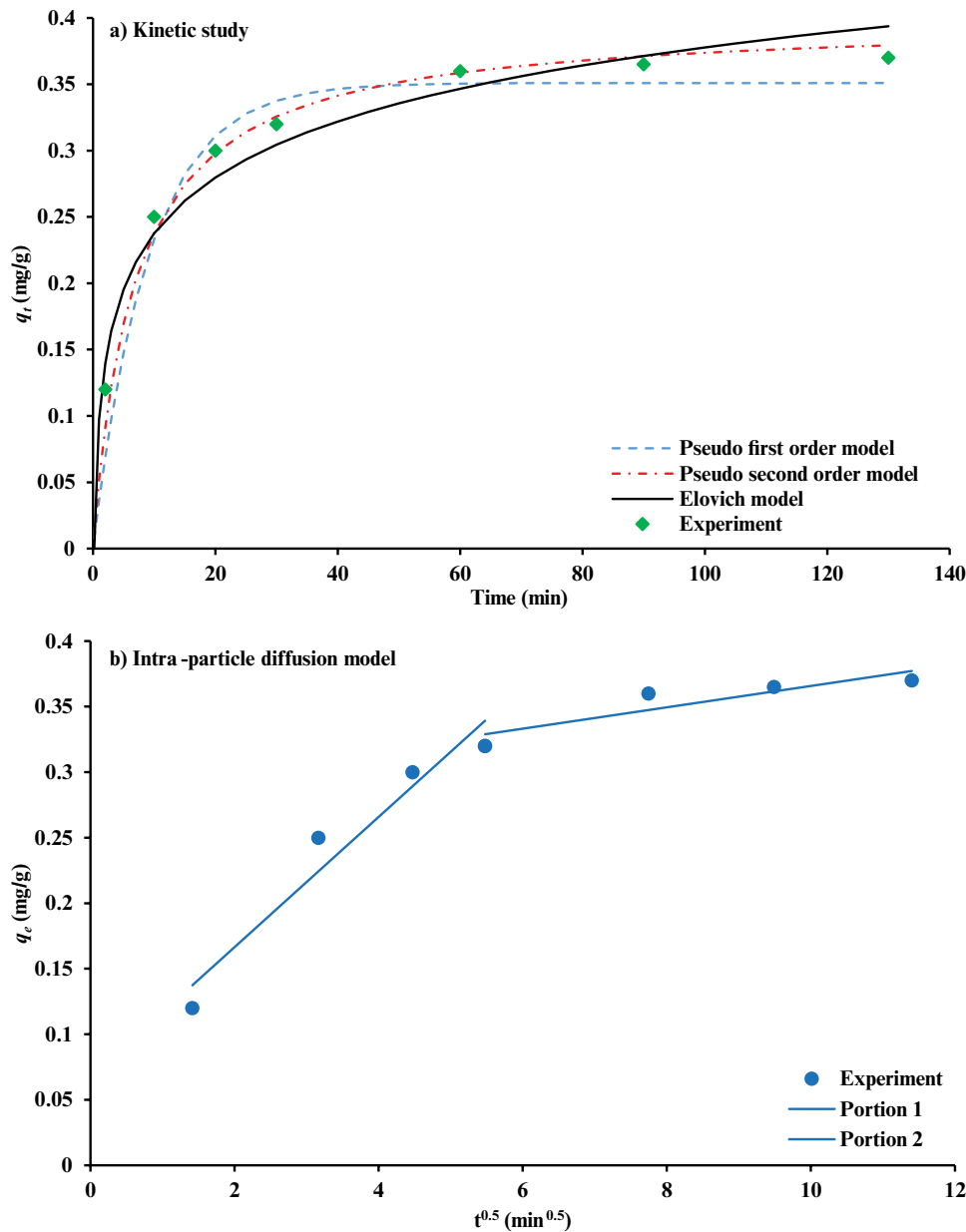


Fig. 2. (a) Kinetic models and (b) intra-particle diffusion model for $\text{NH}_3\text{-N}$ sorption onto WFS (pH = 6, speed = 200 rpm, mass of sorbent = 90 g/100 mL, and initial concentration = 476 mg/L).

a value of 0.0497 for the first portion and it was decreased to be 0.0081 for the second portion. The outputs of this model certified that the removal process is governed by both film and pore diffusion with the rate of macro-pore diffusion greater than that of micro-pore diffusion.

4.2. Sorption isotherms

Fig. 3 shows the Freundlich, Langmuir, and Sips models plotted together with experimental measurements for sorption of $\text{NH}_3\text{-N}$ onto WFS after implementation of fitting process based on the same option in the Microsoft Excel mentioned previously. Table 2 lists the values of model parameters; however, the maximum adsorption capacity

was found to be 1.152 mg/g. This Table 2 with Fig. 3 demonstrated that there is a good matching between the measurements and predicted values for removal of $\text{NH}_3\text{-N}$ onto WFS, especially with Langmuir and Sips models.

4.3. Continuous studies

Results of the first configuration (i.e., column packed with a mixture of 60% coarse sand and 40% fine sand) at flow rate and inlet concentration of 25 mL/min and 200 mg/L, respectively, proved that the effluent concentrations of $\text{NH}_3\text{-N}$ were approximately equal to influent concentration for a period not exceeding 80 h at port P2. So, the sand can classify as "inert material". It was just used

to increase the hydraulic conductivity of the barrier beyond mixing it with WFS for column tests. Fig. 4 shows the effect of flow rate on the propagation of NH₃-N front through the column packed with 10% and 20% WFS for second and third configurations, respectively, described previously at the ports P1 and P2 for 700 mg/L inlet concentration. This figure certifies the increase of flow rate from 25 to 35 mL/

min will increase the steepness of the breakthrough curve with a significant reduction in the times required for specifying saturation and breakthrough points. Indeed, this behavior can be explained on the basis that the increase of flowrate means the increase of pore water velocity which is accompanied by decreasing of residence time within the bed; so, this will decrease the opportunity of contaminant molecules capturing [49]. Table 3 presents the breakthrough and saturation times identical to 5% and 95% of normalized concentration for flow rates of 25, 30, and 35 mL/min at inlet concentration of 700 mg/L when the percentage of WFS equal to 10% and 20%.

For a flow rate of 35 mL/min and pH of contaminated water of 9, the breakthrough curves at inlet concentrations of NH₃-N equal to 200, 500, and 700 mg/L for ports P1 and P2 through the beds of 10 and 20% WFS are illustrated in Figs. 5 and 6. It seems that the higher values of applied concentration will lead to an increase of its gradient and

Table 2
Values of parameters for models of NH₃-N sorption onto WFS

Study	Model	Parameter	Value
Kinetic	Pseudo-first-order	q_e (mg/g)	0.352
		k_1 (min ⁻¹)	0.108
		R^2	0.972
	Pseudo-second-order	q_e (mg/g)	0.398
		k_2 (g/mg min)	0.372
		R^2	0.989
	Elovich	β (g/mg)	16.41
		α (mg/g min)	0.301
		R^2	0.929
Freundlich	K_F (mg/g)(L/mg) ^{1/n}	0.076	
	1/n	0.391	
	R^2	0.913	
Sorption isotherm	Langmuir	q_{max} (mg/g)	1.152
		b (L/mg)	0.006
		R^2	0.923
	Sips	K_s (L/mg)	0.003
		a_s (kJ/mol)	1.181
		β_s	0.003
		R^2	0.923

Table 3
Breakthrough and saturation times for NH₃-N sorption on the beds of 10% and 20% WFS for various inlet concentration at pH = 9 and flow rate = 35 mL/min for ports P1 and P2

Location and inlet concentration (mg/L)		Breakthrough time (h)		Saturation time (h)	
		10%	20%	10%	20%
P1	200	7	7.6	18.35	16.75
	500	5.85	6.35	16.5	13.6
	700	3.3	3.6	15.5	10.6
P2	200	53.75	52.6	73.25	80.0
	500	48.85	49.0	64.85	69.5
	700	45.25	45.5	61.85	66.1

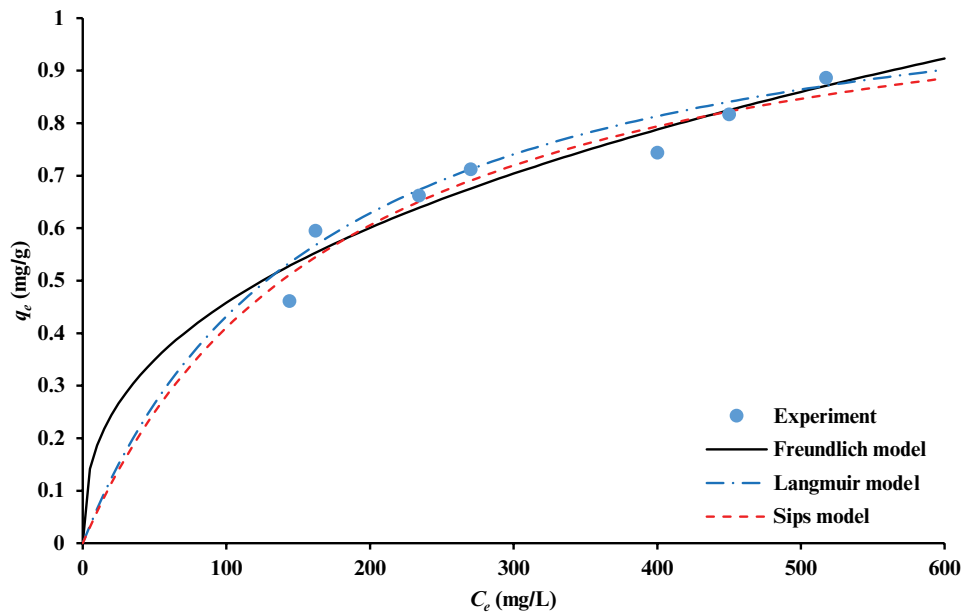


Fig. 3. Isotherm models of NH₃-N sorption onto WFS (pH = 9, time = 120 min, agitation speed = 200 rpm, and initial concentration = 697 mg/L).

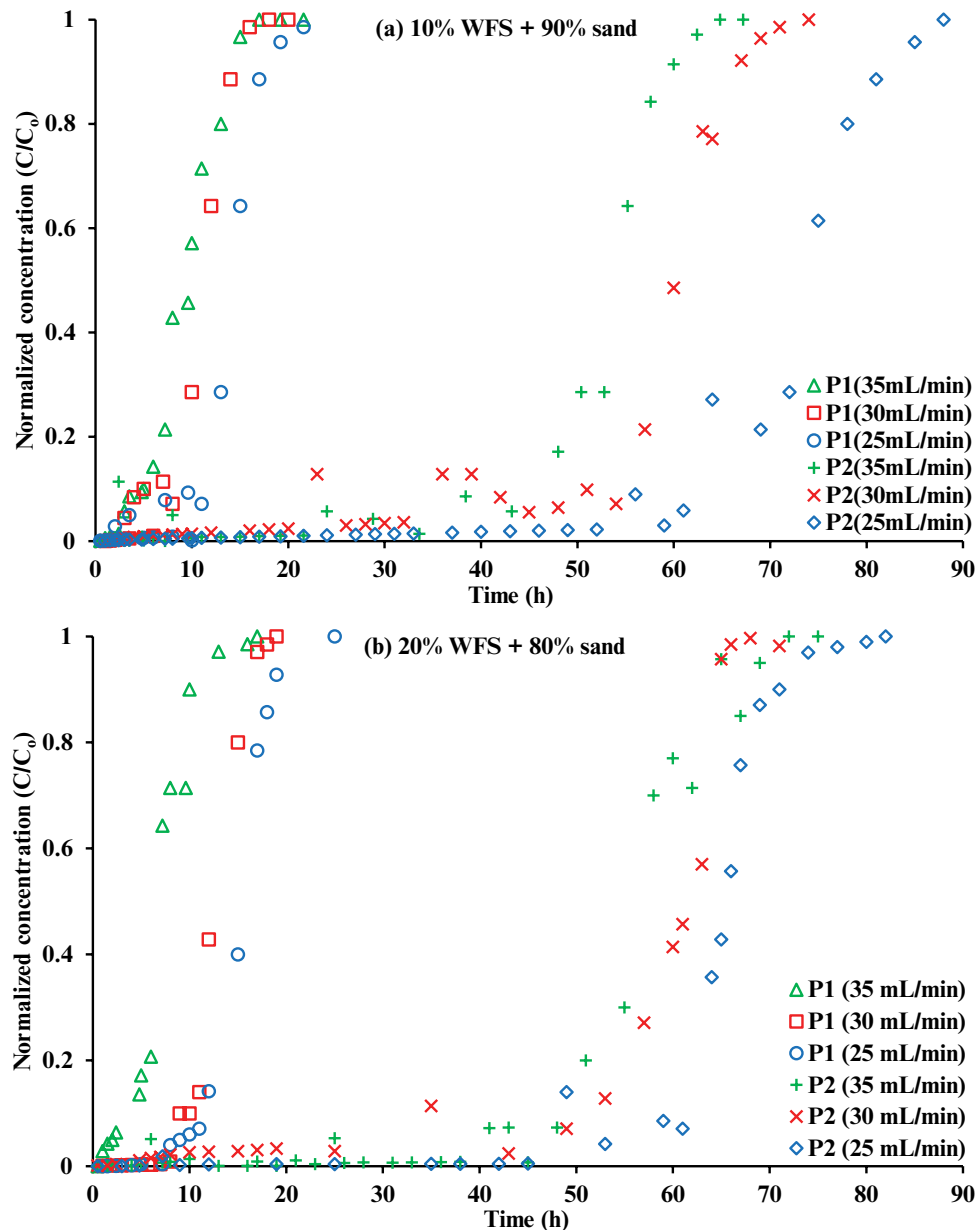


Fig. 4. Breakthrough curves for sorption of $\text{NH}_3\text{-N}$ on the beds of (a) 10% and (b) 20% WFS for various values of flow rate with $\text{pH} = 9$ and $C_0 = 700$ mg/L for ports P1 and P2.

this can accelerate the propagation of contaminant front and, consequently, exhaustion of the bed due to smaller mass transfer resistance. All results signified that the larger beds have high sorption capacities for the same values of flow rate and inlet concentration because this will increase the residence time of contaminant with the packed bed. For example, the increase of bed depth from 15 to 80 cm will be accompanied by an increase of time required to reach the breakthrough point (that identical to C/C_0 of 5%) from 12 to 61 h, respectively, for flowrate 25 mL/min and 10% WFS bed. In addition, the proportions of WFS used in the packed beds proved their activity in maintaining the hydraulic conductivity required for PRB. This may be attributed to the ability of these beds for producing

interconnected pores that not infilling by precipitation products or biological growth. All measurements demonstrated that the increase of WFS proportion in the PRB will cause a clear delay in the appearance of contaminant front due to the increase of retardation factor because of the increment in the value of bulk density for the packed bed.

The finding of a suitable model for representing the relationship between the concentration and residence time introduces insights into the sorption pathways, sorbent characteristics, and sorbent affinity [50]. Accordingly, the familiar models of Thomas, Belter, and Yan were applied to formulate the experimental outputs of the column tests as shown in Figs. 5 and 6. The plotted curves by mentioned models can use effectively in the designing of PRB

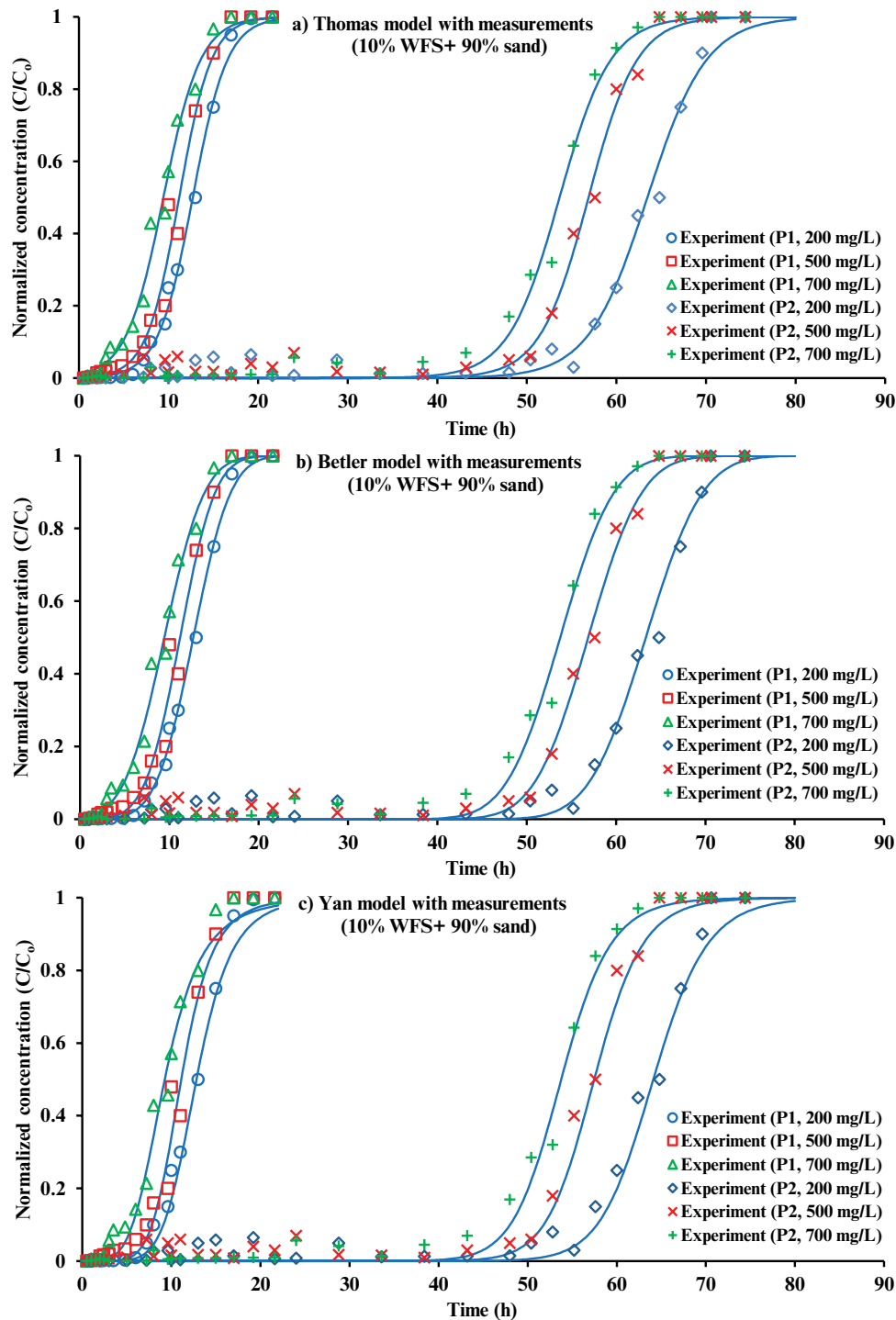


Fig. 5. Measured breakthrough curves with empirical models for the sorption of $\text{NH}_3\text{-N}$ onto the bed consisted of 10% WFS plus 90% sand for various values of inlet concentrations and locations with $\text{pH} = 9$ and flow rate = 35 mL/min.

because they give a clear vision of the migration rate of the contaminant in the selected locations along the laboratory column. This will be required in the determination of bed depth to ensure that the effluent concentration below the acceptable environmental regulation for contaminant under consideration [51]. Consequently, the saturation and breakthrough points can be estimated easily when

finding the more representative model for the measured breakthrough curves. The choosing of a suitable model is depended on the calculated values of Nash–Sutcliffe efficiency (E) and R^2 to find the degree of compliance between the measurements and predicted values. Perfect matching between the predicted and experimental values can achieve when Nash–Sutcliffe efficiency = 1. Table 4

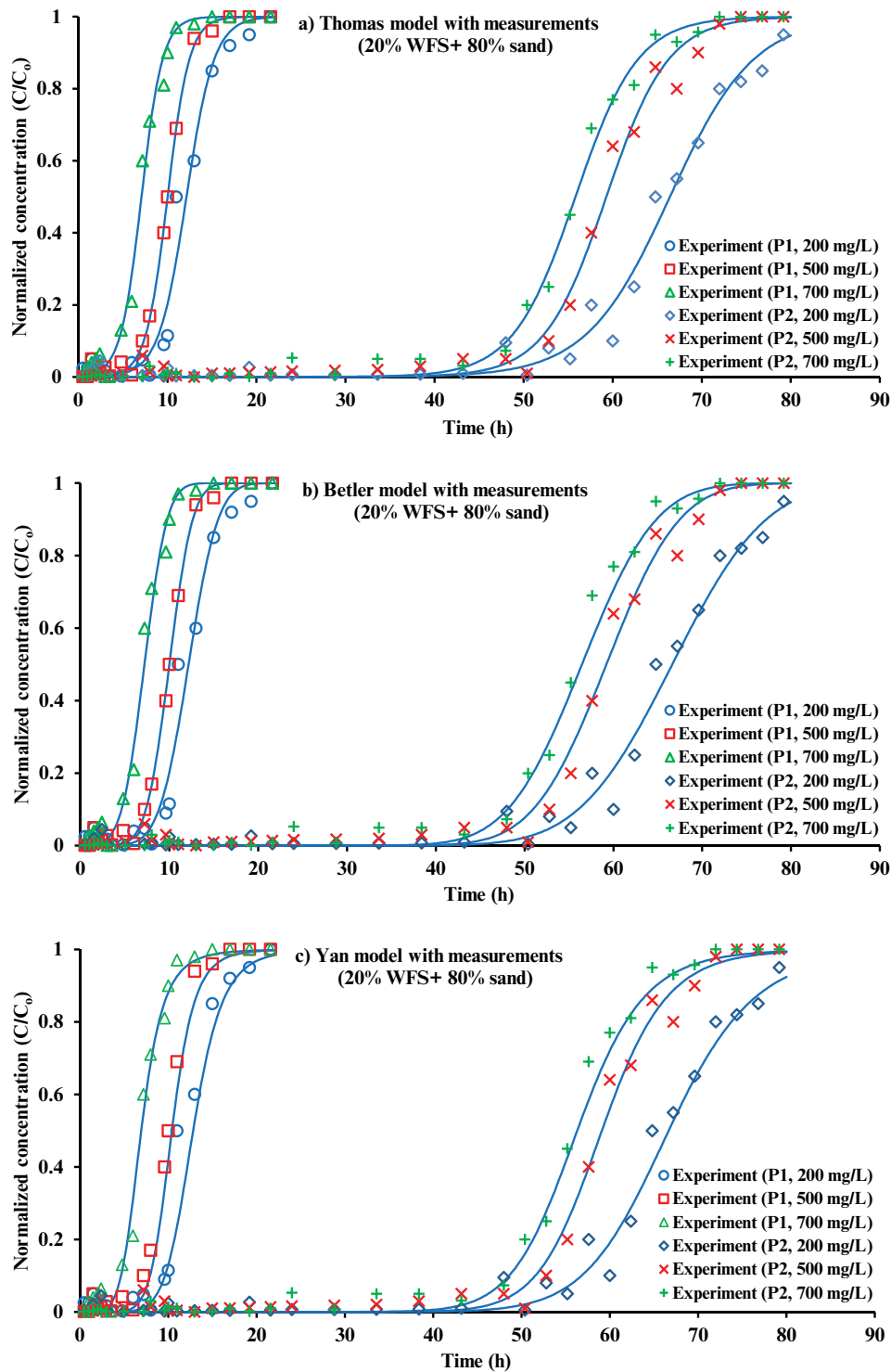


Fig. 6. Measured breakthrough curves with empirical models for the sorption of $\text{NH}_3\text{-N}$ onto bed consisted of 20% WFS plus 80% sand for various values of inlet concentrations and locations with $\text{pH} = 9$ and flow rate = 35 mL/min.

lists the constants of the breakthrough models utilized in this work with statistical goodness parameters. Results of this table in combination with Figs. 5 and 6 certified that all utilized breakthrough models are described in well manner the measured breakthrough curves.

5. Conclusions

Experimental results certified that the WFS resulted as a byproduct from the steel industry could be used effectively in the remediation of water contaminated with

Table 4
 Constants of the Thomas, Belter, and Yan models for beds contained 10% and 20%WFS at different ports and concentrations

Model	Parameter	P1						P2					
		200 mg/L		500 mg/L		700 mg/L		200 mg/L		500 mg/L		700 mg/L	
		10%	20%	10%	20%	10%	20%	10%	20%	10%	20%	10%	20%
Thomas	$\frac{(Mq_0k_{Th})}{Q}$	6.549	7.807	6.200	8.211	4.545	6.007	19.201	14.164	20.959	16.998	18.7713	15.938
	$\frac{K_{Th}C_0}{1000}$	0.5157	0.6431	0.5542	0.8195	0.4819	0.8471	0.3025	0.2132	0.3684	0.2867	0.3498	0.2855
	<i>E</i>	0.997	0.976	0.988	0.990	0.992	0.977	0.956	0.975	0.977	0.987	0.986	0.988
	<i>R</i> ²	0.997	0.981	0.987	0.991	0.991	0.978	0.965	0.977	0.986	0.989	0.988	0.989
	<i>t</i> ^{0.5} (min)	761	730	672	600	566	432	3,800	3,998	3,413	3,553	3,225	3,388
Belter	σ	0.259	0.214	0.275	0.206	0.375	0.279	0.079	0.124	0.083	0.109	0.088	0.116
	<i>E</i>	0.997	0.976	0.987	0.990	0.993	0.974	0.955	0.974	0.977	0.986	0.985	0.987
	<i>R</i> ²	0.997	0.981	0.987	0.992	0.992	0.977	0.965	0.977	0.987	0.989	0.988	0.989
	$\left(\frac{Q \times C_0}{q_0 \cdot M}\right) \times 10^{-3} \left(\frac{1}{\text{min}}\right)$	1.3	1.3	1.5	1.6	1.8	2.4	0.26	0.25	0.29	0.282	0.31	0.296
Yan	<i>a</i>	6.418	7.672	6.269	8.077	4.413	5.49	21.118	13.718	21.103	16.086	19.439	14.918
	<i>E</i>	0.993	0.972	0.983	0.989	0.987	0.980	0.953	0.975	0.976	0.987	0.984	0.988
	<i>R</i> ²	0.994	0.980	0.985	0.991	0.987	0.981	0.964	0.978	0.987	0.990	0.987	0.990

ammoniacal nitrogen. The pseudo-second-order model was more representative in the description of kinetic sorption data and, consequently, chemisorption was the predominant mechanism. Langmuir and Sips models described the equilibrium isotherm sorption measurements in a good manner. The maximum adsorption capacity and affinity constant for the interaction of $\text{NH}_3\text{-N}$ and WFS were equal to 1.152 mg/g and 0.006 L/mg, respectively, at pH = 9, contact time = 120 min, and agitation speed = 200 rpm for an initial concentration of 697 mg/L. Based on the outputs of the intra-particle diffusion model, the sorption process was governed by both pore and film diffusion mechanisms. To prepare the suitable PRB that satisfies the hydraulic conductivity coefficient and reactivity requirements, two mixing ratios of WFS with sand specifically 10:90 and 20:80 were tested. The measurements of the continuous tests with Thomas, Belter, and Yan breakthrough models demonstrated that the bed depth, WFS ratio, flow rate of inflow, and inlet concentration have a remarkable influence on the performance and longevity of the WFS-PRB. An increase of WFS ratio and bed depth in combination with a decrease in flow rate and inlet concentration could produce PRB with high longevity.

Acknowledgments

One of the authors (BS) is grateful to the Taif University Researchers Supporting Project number (TURSP-2020/49), Taif University, Taif, Saudi Arabia for the financial support. Also, the authors would like to gratefully acknowledge the technical support of Environmental Engineering Department/ University of Baghdad during this work.

References

- [1] M. Šiljeg, L. Foglar, M. Kukučka, The ground water ammonium sorption onto Croatian and Serbian clinoptilolite, *J. Hazard. Mater.*, 178 (2010) 572–577.
- [2] J. Ma, Y. Shi, X. Chen, H.X. Wang, Nitrogen load from rural non-point source pollution in suburb area of Shenyang: a case study of Damintun town, *Adv. Mater. Res.*, 610–613 (2012) 3277–3281.
- [3] C. Li, Batch and Bench-Scale Fixed-Bed Column Evaluations of Heavy Metal Removals From Aqueous Solutions and Synthetic Landfill Leachate Using Low-Cost Natural Adsorbents, Queen's University, Kingston ON, 2008.
- [4] H.A. Aziz, M.S. Yusoff, M.N. Adlan, N.H. Adnan, S. Alias, Physico-chemical removal of iron from semi-aerobic landfill leachate by limestone filter, *Waste Manage.*, 24 (2004) 353–358.
- [5] L. Huang, F. Liu, Y. Yang, X. Kong, Y. Zhang, Ammonium-nitrogen contaminated groundwater remediation by a sequential three-zone permeable reactive barrier with oxygen-releasing compound (ORC)/clinoptilolite/spongy iron: column studies, *Environ. Sci. Pollut. Res.*, 22 (2015) 3705–3714.
- [6] M.A. Rahi, A.A.H. Faisal, Performance of subsurface flow constructed wetland systems in the treatment of Al-Rustumia municipal wastewater using continuous loading feed, *Iraqi J. Chem. Pet. Eng.*, 20 (2019) 33–40.
- [7] M.A. Rahi, A.A.H. Faisal, L.A. Naji, S.A. Almutkar, S.N. Abed, M. Scholz, Biochemical performance modelling of non-vegetated and vegetated vertical subsurface-flow constructed wetlands treating municipal wastewater in hot and dry climate, *J. Water Process Eng.*, 33 (2020) 101003, doi: 10.1016/j.jwpe.2019.101003.
- [8] B.J. Bedah, A.A.H. Faisal, Use of vertical subsurface flow constructed wetland for reclamation of wastewater contaminated with Congo red dye, *Plant Arch.*, 20 (2020) 8784–8792.
- [9] M. Wei, F. Harnisch, C. Vogt, J. Ahlheim, T. Neu, H. Richnow, Harvesting electricity from benzene and ammonium-contaminated groundwater using a microbial fuel cell with an aerated cathode, *RSC Adv.*, 5 (2015) 5321–5330.
- [10] Y. Wang, S. Liu, Z. Xu, T. Han, S. Chuan, T. Zhu, Ammonia removal from leachate solution using natural Chinese clinoptilolite, *J. Hazard. Mater.*, 136 (2006) 735–740.
- [11] C. Della Rocca, V. Belgiorno, S. Meriç, Overview of in-situ applicable nitrate removal processes, *Desalination*, 204 (2007) 46–62.
- [12] R. Thiruvenkatachari, S. Vigneswaran, R. Naidu, Permeable reactive barrier for groundwater remediation, *J. Ind. Eng. Chem.*, 14 (2008) 145–156.
- [13] A.D. Henderson, A.H. Demond, Long-term performance of zero-valent iron permeable reactive barriers: a critical review, *Environ. Eng. Sci.*, 24 (2007) 401–423.
- [14] M.I. Aguilar, J. Sáez, M. Lloréns, A. Soler, J.F. Ortuño, Nutrient removal and sludge production in the coagulation–flocculation process, *Water Res.*, 36 (2002) 2910–2919.
- [15] T. Van Nooten, L. Diels, L. Bastiaens, Design of a multifunctional permeable reactive barrier for the treatment of landfill leachate contamination: laboratory column evaluation, *Environ. Sci. Technol.*, 42 (2008) 8890–8895.
- [16] H. Huang, X. Xiao, B. Yan, L. Yang, Ammonium removal from aqueous solutions by using natural Chinese (Chende) zeolite as adsorbent, *J. Hazard. Mater.*, 175 (2010) 247–252.
- [17] S. Ahsan, S. Kaneco, K. Ohta, T. Mizuno, K. Kani, Use of some natural and waste materials for waste water treatment, *Water Res.*, 35 (2001) 3738–3742.
- [18] M. Sarioglu, Removal of ammonium from municipal wastewater using natural Turkish (Dogantepe) zeolite, *Sep. Purif. Technol.*, 41 (2005) 1–11.
- [19] M. Naushad, Z.A. Allothman, M.R. Awual, M.M. Alam, G.E. Eldesoky, Adsorption kinetics, isotherms, and thermodynamic studies for the adsorption of Pb_{2+} and Hg_{2+} metal ions from aqueous medium using Ti(IV) iodovanadate cation exchanger, *Ionics*, 21 (2015) 2237–2245.
- [20] M. Naushad, A. Mittal, M. Rathore, V. Gupta, Ion-exchange kinetic studies for Cd(II), Co(II), Cu(II), and Pb(II) metal ions over a composite cation exchanger, *Desal. Water Treat.*, 54 (2015) 2883–2890.
- [21] M. Naushad, Z.A. Allothman, Separation of toxic Pb^{2+} metal from aqueous solution using strongly acidic cation-exchange resin: analytical applications for the removal of metal ions from pharmaceutical formulation, *Desal. Water Treat.*, 53 (2015) 2158–2166.
- [22] M. Naushad, Surfactant assisted nano-composite cation exchanger: development, characterization and applications for the removal of toxic Pb^{2+} from aqueous medium, *Chem. Eng. J.*, 235 (2014) 100–108.
- [23] S. Muthusarayanan, N. Sivarajasekar, J.S. Vivek, T. Paramasivan, M. Naushad, J. Prakashmaran, V. Gayathri, O.K. Al-Duajj, Phytoremediation of heavy metals: mechanisms, methods and enhancements, *Environ. Chem. Lett.*, 16 (2018) 1339–1359.
- [24] G. Sharma, D. Pathania, M. Naushad, N.C. Kothiyal, Fabrication, characterization and antimicrobial activity of polyaniline Th(IV) tungstomolybdophosphate nanocomposite material: Efficient removal of toxic metal ions from water, *Chem. Eng. J.*, 251 (2014) 413–421.
- [25] G. Sharma, M. Naushad, Adsorptive removal of noxious cadmium ions from aqueous medium using activated carbon/zirconium oxide composite: isotherm and kinetic modelling, *J. Mol. Liq.*, 310 (2020) 113025, doi: 10.1016/j.molliq.2020.113025.
- [26] A.H. Sulaymon, A.A.H. Faisal, Q.M. Khalief, Cement kiln dust (CKD)-filter sand permeable reactive barrier for the removal of Cu(II) and Zn(II) from simulated acidic groundwater, *J. Hazard. Mater.*, 297 (2015) 160–172.
- [27] A.A.H. Faisal, Effect of pH on the performance of olive pips reactive barrier through the migration of copper-contaminated groundwater, *Desal. Water Treat.*, 57 (2016) 4935–4943.

- [28] A.A.H. Faisal, Z.S. Nassir, L.A. Naji, M. Naushad, T. Ahamad, A sustainable approach to utilize olive pips for the sorption of lead ions: numerical modeling with aid of artificial neural network, *Sustainable Chem. Pharm.*, 15 (2020) 100220, doi: 10.1016/j.scp.2020.100220.
- [29] M.H. Rashid, A.A.H. Faisal, Removal of dissolved cadmium ions from contaminated wastewater using raw scrap zero-valent iron and zero valent aluminum as locally available and inexpensive sorbent wastes, *Iraqi J. Chem. Pet. Eng.*, 19 (2018) 39–45.
- [30] H. Rashid, A. Faisal, Removal of dissolved trivalent chromium ions from contaminated wastewater using locally available raw scrap iron-aluminum waste, *Al-Khwarizmi Eng. J.*, 15 (2019) 134–143.
- [31] P.E.F. Oliveira, L.D. Oliveira, J.D. Ardisson, R.M. Lago, Potential of modified iron-rich foundry waste for environmental applications: Fenton reaction and Cr(VI) reduction, *J. Hazard. Mater.*, 194 (2011) 393–398.
- [32] H. Zheng, D. Liu, Y. Zheng, S. Liang, Z. Liu, Sorption isotherm and kinetic modeling of aniline on Cr-bentonite, *J. Hazard. Mater.*, 167 (2009) 141–147.
- [33] A.A.H. Faisal, I.M. Ali, L.A. Naji, H.M. Madhloom, N. Al-Ansari, Using different materials as permeable reactive barrier for remediation of groundwater contaminated with landfill's leachate, *Desal. Water Treat.*, 175 (2020) 152–163.
- [34] A.A.H. Faisal, S.F.A. Al-Wakel, H.A. Assi, L.A. Naji, M. Naushad, Waterworks sludge-filter sand permeable reactive barrier for removal of toxic lead ions from contaminated groundwater, *J. Water Process Eng.*, 33 (2020) 101112, doi: 10.1016/j.jwpe.2019.101112.
- [35] D.N. Ahmed, L.A. Naji, A.A.H. Faisal, N. Al-Ansari, M. Naushad, Waste foundry sand/MgFe-layered double hydroxides composite material for efficient removal of Congo red dye from aqueous solution, *Sci. Rep.*, 10 (2020) 2042, doi: 10.1038/s41598-020-58866-y.
- [36] K. Balasubramani, N. Sivarajasekar, M. Naushad, Effective adsorption of antidiabetic pharmaceutical (metformin) from aqueous medium using graphene oxide nanoparticles: Equilibrium and statistical modelling, *J. Mol. Liq.*, 301 (2020) 112426, doi: 10.1016/j.molliq.2019.112426.
- [37] M. Gheju, A. Miulescu, Sorption equilibrium of hexavalent chromium on granular activated carbon, *Chem. Bull. Polytechnica Univ.*, 52 (2007) 1–2.
- [38] K.Y. Foo, B.H. Hameed, Insights into the modeling of adsorption isotherm systems, *Chem. Eng. J.*, 156 (2010) 2–10.
- [39] G.P. Jeppu, T.P. Clement, A modified Langmuir–Freundlich isotherm model for simulating pH-dependent adsorption effects, *J. Contam. Hydrol.*, 129–130 (2012) 46–53.
- [40] L.K. Wang, Y.T. Hung, S.T.L. Tay, J.H. Tay, *Environmental Bioengineering, Part of the Handbook of Environmental Engineering Book Series*, Vol. 11, Springer, Totowa, New Jersey, ISBN 978-1-58829-493-7, 2010.
- [41] W. Weber, J. Morris, *Advances in Water Pollution Research: Removal of Biologically Resistant Pollutant from Waste Water by Adsorption, Proceedings of the International Conference on Water Pollution Symposium*, Oxford, Pergamon, 1962, pp. 231–266.
- [42] F.-C. Wu, R.-L. Tseng, R.-S. Juang, Comparisons of porous and adsorption properties of carbons activated by steam and KOH, *J. Colloid Interface Sci.*, 283 (2005) 49–56.
- [43] R. Siddiquea, G. Kaur, A. Rajor, Waste foundry sand and its leachate characteristics, *Resour. Conserv. Recycl.*, 54 (2010) 1027–1036.
- [44] N. Moraci, S. Bilardi, P.S. Calabrò, Critical aspects related to Fe⁰ and Fe⁰/pumice PRB design, *Environ. Geotech.*, 3 (2016) 114–124.
- [45] G.O. El-Sayed, H.A. Dessouki, S.S. Ibrahim, Bio-sorption of Ni(II) and Cd(II) ions from aqueous solutions onto rice straw, *Chem. Sci. J.*, 9 (2010) 1–11.
- [46] A.A.H. Faisal, Z.A. Hmood, Groundwater protection from cadmium contamination by zeolite permeable reactive barrier, *Desal. Water Treat.*, 53 (2015) 1377–1386.
- [47] I. Campos, J. Álvarez, P. Villar, A. Pascual, L. Herrero, Foundry sands as low-cost adsorbent material for Cr(VI) removal, *Environ. Technol.*, 34 (2013) 1267–1281.
- [48] B.M.W.P.K. Amarasinghe, R.A. Williams, Tea waste as a low cost adsorbent for the removal of Cu and Pb from wastewater, *Chem. Eng. J.*, 132 (2007) 299–309.
- [49] D.C.K. Ko, J.F. Porter, G. McKay, Optimised correlations for the fixed-bed adsorption of metal ions on bone char, *Chem. Eng. Sci.*, 55 (2000) 5819–5829.
- [50] K.Y. Foo, L.K. Lee, B.H. Hameed, Preparation of tamarind fruit seed activated carbon by microwave heating for the adsorptive treatment of landfill leachate: a laboratory column evaluation, *Bioresour. Technol.*, 133 (2013) 599–605.
- [51] S. Bilardi, P.S. Calabrò, N. Moraci, The removal efficiency and long-term hydraulic behaviour of zero valent iron/lapillus mixtures for the simultaneous removal of Cu²⁺, Ni²⁺ and Zn²⁺, *Sci. Total Environ.*, 675 (2019) 490–500.